JOURNAL OF CATALYSIS 43, 304–321 (1976)

Effect of Ultraviolet Radiation on Zinc Oxide Catalysts

W. R. MURPHY,[1] T. F. VEERKAMP,[2] AND T. W. LELAND

Department of Chemical Engineering, Rice University, Houston, Texas 77001

Received July 11, 1975

The effect of monochromatic irradiation on the powdered zinc oxide catalyst used in heterogeneous catalytic reactions of hydrogen with deuterium and of carbon monoxide with oxygen has been studied. No photocatalytic effect for the H_2–D_2 exchange reaction was observed for radiation with wavelengths from 2000 to 8000 Å when accompanying thermal effects are eliminated. In contrast, marked effects with regard to rate and kinetics were observed for the carbon monoxide oxidation reaction between 30 and 350°C during irradiation with wavelengths corresponding to an energy equal to or in excess of the band gap of the semiconductor. The effect on the two reactions of monochromatic radiation at various frequencies but constant intensity is analyzed in terms of the reaction mechanisms, and the electronic state of the catalyst surface.

INTRODUCTION

Electronic aspects of heterogeneous catalysis may be studied by measuring the effects of monochromatic electromagnetic radiation with a photon energy corresponding to that of an electronic transition within the catalyst. Identification of reaction mechanisms is then assisted by correlating photocatalytic effects with changes in the electronic states of the catalyst. The mechanism of the H_2–D_2 exchange over MgO has previously been studied by this method in this laboratory (*1*). This paper describes an improvement in this technique which allows electronic effects of the irradiation to be separated from thermal effects and eliminates consequences of varying radiation intensity. It is applied to two reactions catalyzed by zinc oxide, specifically the H_2–D_2 exchange and the oxidation of CO.

Several studies (*2–8*) have been made of the oxidation of CO over irradiated zinc oxide which report the existence of photocatalytic effects. The CO oxidation study in this work is an extension and refinement of the work of Romero-Rossi and Stone (*3*). Their study definitely showed an enhancement of the oxidation rate by ultraviolet irradiation and also indicated the existence of a frequency effect. However, only three different frequencies were studied and it is not entirely clear to what extent the observed rate changes were influenced by intensity variations in the incident radiation. This work presents a more quantitative determination of the frequency dependence and examines it over a much wider range of temperatures and compositions. Furthermore, a study has been made of the effect of ultraviolet irradiation on the poisoning produced by the CO_2 reaction product.

Photoenhancement of the H_2–D_2 exchange over ZnO is reported in only one investigation (*9*), although several doping (*10*) and pretreatment (*11*) experiments have suggested that changes in the electronic structure of ZnO should modify the exchange reaction. Although the initial

---

[1] Present address: Mobil Research and Development Corp. P. O. Box 1025, Princeton, New Jersey 08540.

[2] Present address: E. I. DuPont Co., Inc., 1007 Market St., Wilmington, Delaware 19898.

objective was to obtain a more quantitative measurement and to study the frequency dependence of the rate enhancement reported by Freund (*9*), the findings of this study differ completely in that they show no radiation induced changes when thermal effects are eliminated. An objective of this study is to explain the strong photoenhancement of the CO oxidation rate and its absence in the case of the H_2–D_2 exchange and to compare the role of electronic properties of ZnO in each case.

EXPERIMENTAL METHODS

The catalytic material was powdered SP-500 zinc oxide (New Jersey Zinc Co.) with a nitrogen BET surface of 2.2 m^2/g regardless of the pretreatment. The radiation source was a mercury lamp (Osram, HBO 200 W) and a Bausch and Lomb monochromator continuously tunable from 2000 to 8000 Å.

Deuterium, carbon monoxide, and oxygen were obtained from the Liquid Carbonic Co., hydrogen and carbon dioxide from The Matheson Co. The CO_2 was purified by passing over magnesium perchlorate and through a glass-bead filled trap cooled with dry ice and acetone. Carbon monoxide and oxygen were similarly purified with the trap cooled with liquid nitrogen. Hydrogen and deuterium were diffused through an Engelhard HPD-0-50 paladium thimble before preparation of the equimolar reactant mixtures.

The reaction vessel for the H_2–D_2 exchange reaction has been described in detail elsewhere (*1*). It consisted of a 1.5 in. diameter Pyrex tube with a 0.25 in. thick, optically flat Supersil-II quartz window fused to the bottom. ZnO (1.0 g) was spread evenly on the window and heated to the required temperature by an open-ended electric furnace which extended 1 in. below the bottom of the reaction vessel. The reaction vessel was attached to a recirculation system containing a magnetic pump. After a measured contact time, the reaction mixture was expanded into an evacuated sampling system and analyzed by a CEC 21-104 mass spectrometer.

A similar reaction vessel shown in Fig. 1 was used for the CO oxidation. The ZnO catalyst was spread on the quartz window and heated by means of an electric furnace. Catalyst temperatures were monitored by a thermocouple suspended in a thin walled thermowell located just above the Supersil window and surrounded by the catalyst powder. The system is, in effect, a convection loop with circulation created by the temperature differential between the heated region around the catalyst and the liquid-nitrogen cooled region inside the Dewar. This system was found to be efficient in removing the CO_2 product, which is a strong poison for the dark reaction.

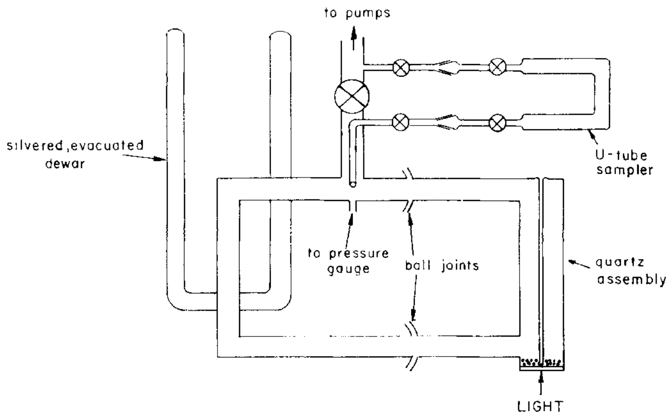

FIG. 1. Diagram of apparatus for CO oxidation study.

Reaction rates were determined by measuring the drop in pressure with time by means of a Bourdon-type gage (Texas Instruments precision pressure gage) and checked by using the CEC mass spectrometer to analyze samples at varying reaction times. The rates in moles per unit time were calculated from the measured rates of change in pressure by using the results of a separate calibration experiment.

Adsorption isotherms of each pure reactant in the dark and during irradiation of the ZnO were determined by measuring the pressure decrease with the Texas Instruments gage and calculating the moles adsorbed from the known temperature and volume of the vessel.

Radiation from the monochromator was reflected through the Supersil window into the reaction cells by means of front surface aluminum mirrors. Light intensities were measured with an internally calibrated thermopile (Hewlett-Packard radiant flux meter 8330/8334). With the thermopile detector in the equivalent catalyst position, the radiant flux on the catalyst was found to be about 36% of the flux directly leaving the monochromator. Calibration graphs of the intensity versus the wavelength of light emitted from the monochromator were prepared.

The source intensity peak which occurred at the energy nearest the 3.2 eV band gap for ZnO happeneed to fall at 3650 Å (~3.4 eV). Since the band pass in this frequency range was 170 Å (~0.16 eV), the radiation tuned to this wavelength coincided closely with the ZnO band gap. The incident flux density on the catalyst with this monochromator setting was about 7 mW/cm^2. This light will be referred to more simply as band gap irradiation in subsequent sections.

Particular care must be taken to develop pretreatment conditions which reactivate the catalyst in a reproducible manner. After a rate measurement at each frequency the catalyst must be regenerated with this pretreatment technique.

RESULTS

The Photocatalyzed Oxidation of Carbon Monoxide

The standard catalyst pretreatment for the CO oxidation experiments entailed heating the ZnO at 300°C in 100 Torr O_2, followed by evacuation, generally below 5×10^{-7} Torr, for 30 min at the reaction temperature before admission of the reaction mixture. At the end of each experiment the reaction cell was evacuated for 10 min (10^{-6} Torr) at 300°C, followed by the addition of oxygen (100 Torr) for at least 4 hr before reducing the catalyst temperature in preparation for a subsequent measurement. This treatment produced approximately a constant dark rate reaction. The dark reaction rate was a sensitive function of pretreatment and reproducible results were obtained only when the time and conditions of oxygen pretreatment at 300°C were carefully duplicated.

Three conditions of reaction were studied. These were:

I. Unirradiated, with CO_2 trapped out in the liquid N_2 trap.

II. Irradiation at an energy corresponding to the ZnO band gap, with CO_2 trapped out in the liquid N_2 trap.

III. Band gap radiation with CO_2 remaining in the gas phase (no liquid nitrogen in the cold trap).

The pressure dependence of the rate data was fitted to a general empirical equation for the reaction rate, r:

$$r = k(P_{CO})^m(P_{O_2})^n(P_{CO_2})^q. \qquad (1)$$

The exponent q in Eq. (1) was found to be zero for the Type III reaction above about 3 Torr of CO_2. It was assumed to be zero also for conditions I and II, although there was evidence of an immeasurably small q value (*12*) at these conditions. The constants m and n were obtained by independently varying the CO and O_2 partial pressures. The results are shown in Table 1. At 200°C these exponents were constant over the pressure range studied, up to about 50 Torr. Table 2 shows the comparative reaction rates at 200°C for one set of partial pressures. These results are the averages of many different runs. Even though the catalyst pretreatment conditions were held as constant as possible, it was difficult to reproduce the rate data on successive determinations.

The effect of temperature is shown in the Arrhenius-type plots in Fig. 2 for the rate constant from Eq. (1) for a typical run at conditions I and III. For the dark rate under condition I an apparent activation energy of 21 kcal/g mole is indicated by the slope. Published values from similar plots for the dark catalyzed reaction (*13*, *14*) vary from 14 to 28 kcal/g mole.

There is generally poor agreement among various investigators (*3*, *14–17*) in regard to the kinetic description of the reaction in terms of the exponents in Eq. (1). The dark rate results for condition I resemble most closely those reported by Romero-Rossi and Stone (*3*) who report first order dependence on the pressure of oxygen. Chizhikova (*13*) showed a strong dependence of the exponent m on the impurity content of the ZnO. The results in Table 1, however, agree with the findings of Tanaka and Blyholder (*4*) in showing that the kinetic behavior of the irradiated reaction is totally different from that of the dark reaction.

TABLE 1

Constants for the rate of CO oxidation over ZnO at 200°C[a]

Reaction condition	Constants[b]		
	m	n	k_{CO}
I Dark rate with CO_2 trapping	0.9	0.1	1.42×10^{13}
II Band gap irradiation with CO_2 trapping	0.45	0.3	9.55×10^{13}
III Band gap irradiation with no CO_2 trapping, $P_{CO_2} > 3$ Torr, $P_{CO} > 20$ Torr	~0.0	0.55	14.95×10^{13}
IV Dark rate with no CO_2 trapping	—	—	~0.0

[a] In the rate equation $r_{CO} = k_{CO}(P_{CO})^m(P_{O_2})^n$.

[b] For CO oxidation rate (molecules/sec/g catalyst) with pressures (Torr).

Spectral Response for the CO Oxidation

Figure 3 shows the effects of variation in intensity of radiation at a fixed wavelength on the condition III reaction rate at 200°C. The fixed wavelength is that of the band gap radiation and the total initial pressure is 83 Torr with CO, CO_2, and O_2 in the partial pressure ratio 2:2:1, respectively. Light intensities were varied by means of calibrated wire screens and a neutral density filter. Each intensity was measured using the radiant flux meter and quantum efficiencies were calculated by assuming

TABLE 2

Comparative Reaction Rates for CO Oxidation over ZnO at 200°C

Reaction conditions[a]	P_{O_2} Torr	P_{CO} Torr	P_{CO_2} Torr	CO oxidation rate	
				g moles/cm²/sec	Molecules/g-catalyst/sec
I	16.6	33.2	~0	3.3×10^{-14}	4.4×10^{14}
II	16.6	33.2	~0	8.1×10^{-14}	10.7×10^{14}
III	16.6	33.2	33.2	5.3×10^{-14}	7.0×10^{14}
IV	16.6	33.2	33.2	~0.0	~0.0

[a] As defined in Table I.

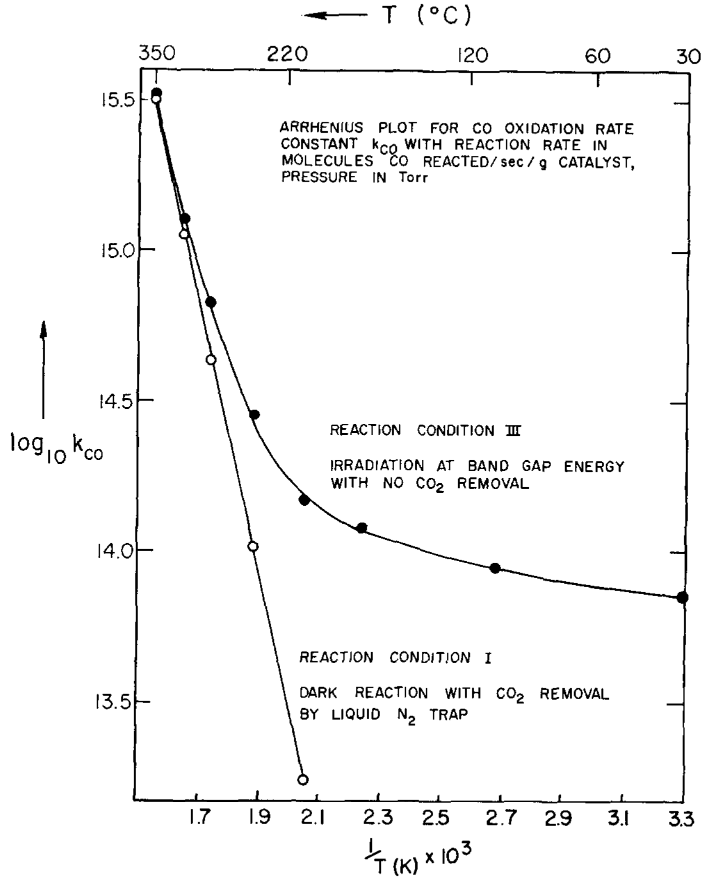

FIG. 2. Irradiation effects on the rate constant of Eq. (1).

that one photon was required for the enhanced oxidation of each CO molecule. As shown in Fig. 3, the quantum efficiency decreases from about 14% to about 6% with increasing light intensity.

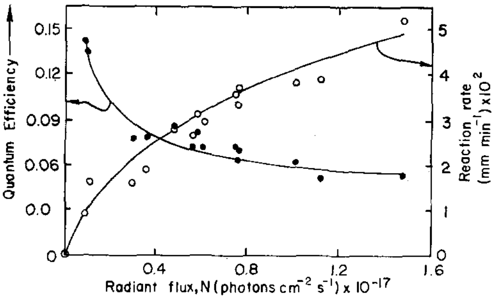

FIG. 3. Quantum efficiency of the photocatalysis of CO oxidation on ZnO.

Figure 3 also shows that the photo-induced reaction rate never becomes independent of the intensity even at the highest attainable radiant fluxes. In the previous study of MgO (*1*) it was found that complete independence of intensity was easily achieved for most active wavelengths, even when employing light sources of lower intensity than used in this present work. This independence was ascribed to the excitation of all possible electron state transitions corresponding to the particular energy of the incident photons. The fact that a similar saturation was not found for ZnO indicates that electron transfers between all the possible donors and acceptors did not occur and implies a much greater decay rate of the excited electron states.

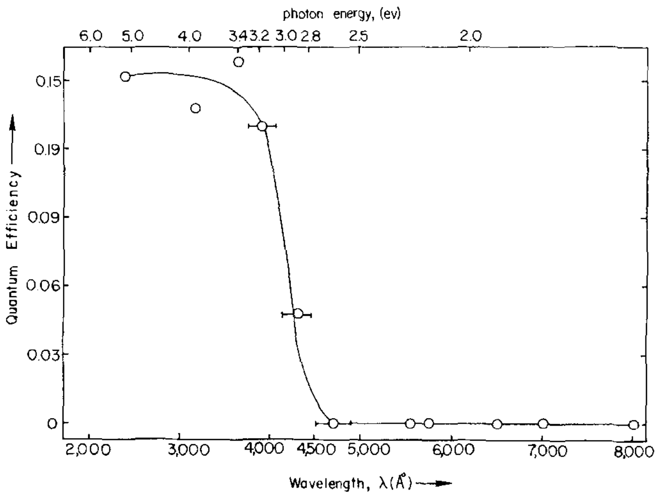

FIG. 4. Dependence of photocatalysis of CO oxidation on wavelength of incident radiation.

Photoenhancement of ZnO occurred only during the irradiation, whereas the excitations in MgO persisted in some cases for many hours after the irradiation was stopped. This is consistent with the observation of Gobrecht *et al.* (*15*) that the luminescent decay time for ZnO following excitation with band gap radiation is only a small fraction of a second.

As a consequence, it is essential to study the spectral response of ZnO catalysts at equal flux densities for each incident wavelength studied. Flux densities at the various wavelengths were regulated with the screens and filters to be equal to that of a peak in the source which happened to occur at 2400 Å, corresponding to about 3.5×10^{15} quanta/cm^2/sec leaving the monochromator. Since 64% of this was lost in the mirror system and quartz window, the spectral response measurements were conducted at a uniform flux density of about 1.3×10^{15} quanta/cm^2/sec at the catalyst surface.

The results for conditions III at 200°C using the 2:2:1 mixture of CO, CO_2, and O_2 at a total of 83 Torr are shown in Fig. 4. The error bars indicate the band pass of the monochromator. The experimental location of the sharp increase in photoresponse, called the "reaction edge," is less well defined than corresponding published data for the ultraviolet absorption edge in ZnO because of the low resolution of the light source and inaccuracies in the rate measure-

TABLE 3

Effects of Pretreatment by Vacuum Heating on the H_2–D_2 Exchange Rate

Temp (°C)	Exposure time	Initial reaction rate constant at 40°C, k_{HD} (av of 3) (g^{-1} min^{-1})
350	0	0
350	1 hr	Catalyst destroyed
300	0	<0.001
300	1 hr	0.021
300	2 hr	0.117
300	6 hr	0.297
300	12 hr	0.339
300	3 days	0.343
250	0	<0.001
250	2 hr	0.050
250	12 hr	0.173
250	3 days	0.327
250	1 week	0.338
200	0	<0.001
200	1 week	0.279
200	2 weeks	0.328
200	1 month	0.340
100	0	<0.001
100	1 week	0.009

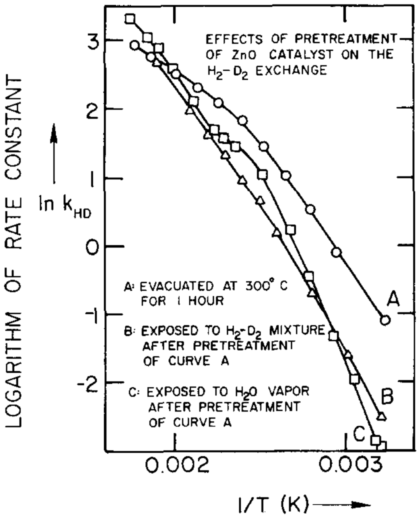

FIG. 5. Pretreatment effects on the rate constant of Eq. (2).

ment. In order to determine the reaction edge more accurately, light of greater resolution with the band pass reduced to 96 Å was also studied. In this case, however, intensity requirements allowed only wavelengths at peak source intensity to be studied. From all of these measurements, the experimental reaction edge is definitely in the spectral region from (4000 − 48) to (4350 + 48) Å or between 3.14 and 2.82 eV. Averaging these extremes locates the reaction edge at about 3.0 eV, in close correspondence to the usually reported band gap energy of 3.2 eV (*16*).

The H_2–D_2 Exchange and Effects of Irradiation

This reaction was studied with an equimolar reactant mixture at temperatures from 25 to 300°C in the pressure range 1–100 Torr with the catalyst irradiated by wavelengths from 2000 to 8000 Å after various pretreatments. First order kinetics for HD production was assumed with the rate constant described by Eq. (2), as derived previously (*1, 17*)

$$k_{HD} = -\frac{\ln[1 - (1 + 2K_{eq}^{-\frac{1}{2}})X_{HD}]}{t(1 + 2K_{eq}^{-\frac{1}{2}})}. \quad (2)$$

The dark rate over ZnO was found to be very sensitive to the type of catalyst pretreatment. Typical results measured for k_{HD} at 40°C are shown in Table 3 for pretreatment by exposing the catalyst for various time periods to a vacuum of about 10^{-7} Torr. Under these conditions the rate constant is an accurately reproducible function of the pretreatment temperature and exposure time. All measurements reported are for a total pressure of 40 Torr. Arrhenius plots of the rate constants following this type of pretreatment at successively higher pretreatment temperatures with the same exposure time are reproducible and parallel. The highest rates accompany the highest pretreatment temperatures. Exposure for even short periods to this vacuum at 350°C visibly liberated metallic zinc throughout the powder and destroyed the catalyst.

Figure 5 shows the rate effects of different adsorbates placed on the surface after pretreatment in this manner. Curve A was obtained by measuring the initial reaction rate following pretreatment by vacuum exposure for 1 hr at 300°C. Curve B was obtained by following this same pretreatment but then saturating the surface with an H_2–D_2 mixture at the reaction temperature, followed by a 30 sec evacu-

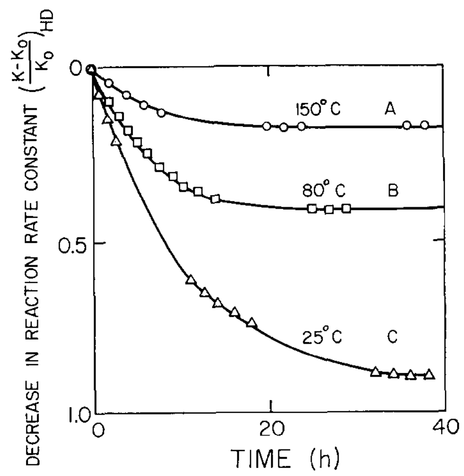

FIG. 6. Decrease of reaction rate of the H_2–D_2 exchange on ZnO due to self-poisoning.

ation before admission of the reactants for rate measurement. Curve C represents the data obtained similarly but with exposure to water vapor at 20 Torr at reaction temperature. An almost identical curve to C was obtained by exposure to oxygen followed by exposure to hydrogen.

Pretreatment by sintering in air at high temperatures was also studied. Catalysts were pretreated by sintering for 24 hr in air at 600, 700, and 800°C. The resulting Arrhenius plots for these pretreatment temperatures are also parallel but the pretreatment temperature effect was reversed from that of the vacuum pretreating. The reaction rate decreased as the pretreatment temperature increased and all reaction rates on these catalysts were much lower than for those pretreated at lower temperatures in vacuum. The qualitative effects of prior exposure to various adsorbates were the same for each type of pretreatment.

None of these pretreatment or surface conditions produced a catalyst in which the rate of reaction was altered in any way by irradiation at any wavelength in the range 2000 to 8000 Å when care was taken to eliminate any thermal effects. The substitution of a less pure grade of ZnO (Baker Analyzed Reagent Grade) also resulted in no response to any radiation following any of these pretreatment procedures. In some cases an apparent enhanced reaction rate was observed when the filtering of accompanying infrared radiation was purposely poor. Subsequent blank experiments employing fine thermocouples embedded in the catalyst showed that these effects were entirely thermal and the observed rate changes corresponded to those calculated by applying the measured temperature change to the Arrhenius plot for the dark rate constant.

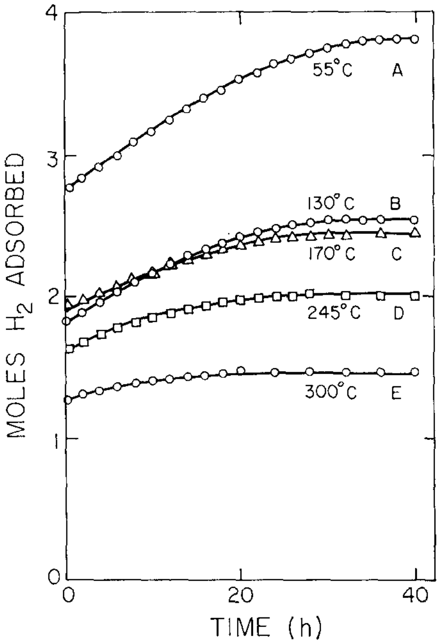

FIG. 7. Adsorption isotherms of H_2 on ZnO.

Self-Poisoning of the H_2–D_2 Exchange

The radiation likewise had no effect on the poisoning of the catalyst by the H_2–D_2 mixture which was observed in this study for the catalysts pretreated by heating in vacuum. As soon as the reactant mixture is admitted to the catalyst the reaction rate starts to decrease. This decrease parallels almost exactly the adsorption of hydrogen or deuterium at the reaction conditions. The reaction rate becomes constant in the same time as required to saturate the surface. The results are shown in Figs. 6 and 7. This poisoning effect occurs at all reaction temperatures as shown by curve B in Fig. 5. Ordinarily one would expect the reaction rate to increase with increased adsorption of the reactants. Tests were performed to insure that these results were not caused by any trace impurities in the reactant gases or by diffusion effects.

Radiation Effects on Adsorption

In studying the photoeffects, a study was also made of the effects of ultraviolet irradiation on the adsorption of hydrogen on the same catalysts and in the same temperature range as used in the reaction studies. When care was taken to eliminate thermal effects there was no radiation effect at any frequency, regardless of the method of pretreatment or impurity content of the ZnO. This result is supported by the work of Tanaka and Blyholder (*4*), who also found no photoeffects on hydrogen adsorption. However, contradictory results are presented by Kesavulu and Taylor (*18*) who reported a decrease in hydrogen adsorption on ZnO on exposure to ultraviolet.

The radiation used in this study gave no evidence of any photodesorption of zinc or oxygen from the zinc oxide itself.

DISCUSSION

Mechanisms for the CO Oxidation

The reaction edge at 3.0 eV is in good agreement with the adsorption edge value of 3.02 eV interpolated from the uv absorption data of Mollwo (*19*). Rubin *et al.* (*20*) measured both the absorption edge and also a reaction edge for the photosynthesis of H_2O_2 over ZnO and found the same energy, about 3.1 eV.

It follows from Fig. 4 therefore, that the primary step in the photocatalysis is the absorption of photons with energy equal to or greater than the absorption edge which produces mobile hole–electron pairs near the surface. From Fig. 4 and from information on the chemisorption of O_2, CO, and CO_2 on ZnO, the role of these hole–electron pairs may be deduced. The first conclusion is that it is the mobile holes formed near the surface which are directly involved in the photocatalytic mechanism and not the electrons. The reasons for this are as follows:

1. There is no catalytic enhancement at any photon energies below the band gap energy, although in impure ZnO there is definitely an enhancement of the electrical conductivity by photons in this energy range (*16*). In this laboratory an unmistakable effect on the conductivity was found to be produced by visible sunlight and reproducible results could not be obtained until the ZnO containing cell was wrapped in foil (*21*). At photon energies below that of the band gap, impurities and defects, such as interstitial zinc, lying within the band gap undergo ionization with the generation of a mobile free electron and a trapped hole remaining at the localized impurity. This produces the observed increase in *n*-type conductivity but no change in reaction rate so that the increase in conduction electrons or trapped holes near the surface has no catalytic effect. However, as soon as additional mobile holes are produced by radiation at the band gap energy, the catalytic enhancement begins at once.

2. Of the three species O_2, CO, and CO_2, the oxygen has by far the strongest chemisorption (*22–25*) forming a negative surface and a positive space charge region with energy band bending, as shown in Fig. 8. Figure 8 represents the electrochemical equilibrium between neutral physically adsorbed oxygen, negatively charged chemisorbed oxygen, and the positive charges in the region just below the surface. The effect of the band gap radiation is to upset this equilibrium by generating additional holes in the valence band and electrons in the conduction band near the surface. Each electron thus generated is unstable at the already strongly negative surface and is repelled into the space charge region where it may be trapped by one of the positive charges. To compensate for this positive charge loss in the space charge region, the negative charge of the surface must also be lowered and the photogenerated hole must remain at the surface to accomplish this. The trapped holes produced by radiation with energy less than the band gap lower this negative charge by remaining at their surface generation sites. Mobile holes, which result from band gap radiation, can lower the surface charge by encountering and reacting with negatively charged surface species and any catalytic changes should be related to this phenomenon.

Electronic Effects of Pretreatment

The type of band diagram shown in Fig. 8 can be created not only by exposure to oxygen but also by pretreatment conditions which involve heating in vacuum. As shown by Amigues and Teichner (*24*) this type of pretreatment leads to a surface decomposition of ZnO. At temperatures above about 350°C metallic zinc can easily be detected in the vacuum system. At lower temperatures this decomposition is confined to the surface layers and much of the displaced zinc remains as interstitials near the surface. Some of the oxygen released either escapes or is physically adsorbed, but depending on the temperature, an appreciable fraction forms chemisorbed negative ions. Electrons for the formation of these ions are obtained largely from the zinc interstitials near the surface which are ionized to Zn^+ creating the positive charge region. In this manner a band diagram like Fig. 8 can be created by vacuum pretreatment as well as by direct oxygen adsorption.

Mechanism for the Dark CO Oxidation

The dark reaction has been studied by several investigators and evidence is now reasonably conclusive that it is catalyzed by two mechanisms. The primary and most rapid of these is that proposed by Amigues and Teichner (*24*), Tanaka and Blyholder (*4*), and Schwab and Block (*14*):

$$O_{(ads)}^- + CO_{(g)} \rightarrow CO_{2(g)} + e^-. \qquad (3)$$

This reaction involves the dominant form of chemisorbed oxygen and accounts for the observed increase in *n*-type conductivity by transfer of the released electron to the conduction band. It is also possible that this primary reaction occurs with a chemisorbed CO^+ molecule with the electron causing the conductivity increase coming from its formation:

$$CO_{(g)} \rightarrow CO_{(ads)}^+ + e^-, \qquad (4)$$

$$O_{(ads)}^- + CO_{(ads)}^+ \rightarrow CO_{2(g)}. \qquad (5)$$

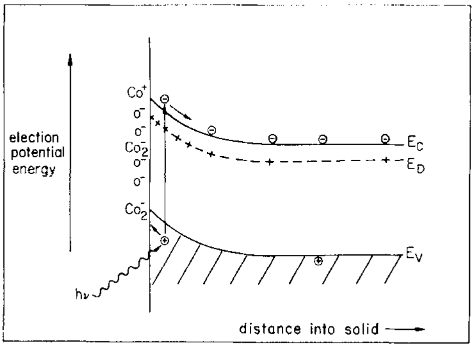

FIG. 8. Band diagram of ZnO with negatively charged surface.

Equations (4) and (5) were proposed by Romero-Rossi and Stone (*3*) and by Komatsu *et al.* (*26*), although the existence of the CO^+ molecule on ZnO is somewhat controversial. A transfer of electrons from the surface to the bulk on CO adsorption has been noted at high temperatures by Amigues and Teichner (*24*), Chon and Prater (*27*), and at room temperature by Amberg and Seanor (*28*). However, because ordinary vacuum pretreating will result in some chemisorbed oxygen the observed conductivity increase could have been due to the electron released by Eq. (3) without the formation of a CO^+ ion. In contradiction to these studies, Doerffler and Hauffe (*2*) reported an opposite electron transfer from the bulk to the surface at 150°C on oxidized ZnO, which could only form a negative species on the surface. All agree, however, that any chemisorption of CO is much weaker than that of oxygen and a high degree of physical adsorption occurs.

In addition to the primary mechanism, most investigators agree that there is a slower secondary mechanism involving other forms of chemisorbed oxygen. Lunsford and Jayne (*29*), Sancier (*23*), and also Chon and Prater (*27*) showed that at room temperature, O_2^- is the dominant chemisorbed species. At higher temperatures, around 160°C according to Tanaka and Blyholder (*4*), this species is replaced by O^- as the dominant form. However Barry and Stone (*30*) and Chon and Prater (*27*) showed that another reactive species, probably an adsorbed O^{2-} ion, is also present and active in the CO oxidation. Amigues and Teichner (*24*) postulated that this secondary mechanism is due to chemisorbed oxygen atoms. The possibilities are, therefore:

$$O_{(ads)}{}^{2-} + CO_{(ads)}{}^{+} \rightarrow CO_{2(g)} + e^{-}, \qquad (6)$$

or

$$O_{(ads)}{}^{2-} + CO_{(g)} \rightarrow CO_{2(g)} + 2e^{-}, \qquad (7)$$

and according to Amigues and Teichner (*24*):

$$O_{(ads)} + CO_{(g)} \rightarrow CO_{2(g)}. \qquad (8)$$

CO_2 Poisoning of the Dark Reaction

The mechanism of the strong CO_2 poisoning action is not entirely clear because of the uncertainty in regard to the chemisorbed form of CO_2, which is apparently strongly dependent on the ZnO pretreatment and preparation. Amigues and Teichner (*24*), who prepared their ZnO from decomposition of $Zn(OH)_2$, report that CO_2 is only physically adsorbed in that it did not modify the conductivity of the sample at any temperature between 25 and 350°C at any pressure below 200 Torr. This same conclusion was reported by Enikeev *et al.* (*25*) at 20°C. However, recent ESR studies by Sancier (*23*) indicated that a CO_3^- species is possible at room temperature. Infrared spectroscopy at high temperatures by Matsushita and Nakata (*31*) showed chemisorption as $O{=}CO_2$, CO_2^-, and CO_3^{2-} on ZnO which was pretreated quite similarly to that used in this work. Creation of these various chemisorbed species could lead to several possible poisoning mechanisms:

1. Reduction of the primary sites by competition for electrons at the surface:

$$e^{-} + \tfrac{1}{2}O_{2(g)} \rightarrow O_{(ads)}{}^{-}, \qquad (9)$$

which competes with

$$e^{-} + CO_{2(g)} \rightarrow CO_{2(ads)}{}^{-}. \qquad (10)$$

2. Removal of the primary sites:

$$O_{(ads)}{}^{-} + CO_{2(g)} \rightarrow CO_{3(ads)}{}^{-}. \qquad (11)$$

3. Removal of secondary sites:

$$O_{(ads)}{}^{2-} + CO_{2(g)} \rightarrow CO_{3(ads)}{}^{2-}, \qquad (12)$$

$$O_{(ads)} + CO_{2(g)} \rightarrow O{=}CO_{2(ads)}. \qquad (13)$$

The Photocatalytic Mechanism

In view of the strong poisoning action of CO_2 one might be led to explain the photoenhancement results in Table 2 by postulating that photodesorption is a more effective way of removing CO_2 from the catalyst than the liquid nitrogen trap. However, a tracer experiment was performed (*32*) to test for radioactivity above a ZnO surface receiving band gap irradiation when the surface had been previously exposed to $C^{14}O_2$. The results showed no photogenerated radioactivity in the gas phase. Stone (*33*) also reports no observable CO_2 desorption from ZnO when irradiated with ultraviolet in this frequency range.

Figure 2 indicates a distinctly different mechanism for the photocatalysis with CO_2 not removed from the system than for the dark reaction with CO_2 removed by the liquid nitrogen trap. In terms of what is known about the various chemisorbed species and the role of mobile holes at the surface, the photocatalysis in the presence of high concentrations of CO_2 can be explained by:

1. Generation of new reaction sites from the adsorbed CO_3 species produced by Eqs. (11) or (12):

$$p^{+} + CO_{3(ads)}{}^{2-} \rightarrow CO_{2(ads)} + O_{(ads)}{}^{-} \qquad (14)$$

or

$$p^{+} + CO_{3(ads)}{}^{-} \rightarrow CO_{2(ads)}{}^{-} + O_{(ads)}. \qquad (15)$$

2. Conversion of a secondary site to a more effective primary site:

$$p^{+} + O_{(ads)}{}^{2-} \rightarrow O_{(ads)}{}^{-}. \qquad (16)$$

3. Increasing the concentration of sites active in the dark reaction:

$$p^+ + CO_{(g)} \rightarrow CO_{(ads)}^+. \qquad (17)$$

4. Enhancement of the primary reaction step [Eq. (3)] by:

$$p^+ + O_{(ads)}^- + CO_g \rightarrow CO_{2g}. \qquad (18)$$

The sites generated in Eqs. (14)–(17) can react according to Eqs. (3)–(5) to cause additional CO oxidation so that any combination of these or Eq. (18) could explain the photocatalysis. Each equation illustrates an effective use of the mobile photogenerated holes concentrated at the surface by the band structure associated with strong oxygen chemisorption.

Adsorption of Hydrogen and Deuterium

A discussion of the H_2–D_2 exchange must begin with the fact that there are several forms of hydrogen and deuterium chemisorption on ZnO. Two of these have been clearly identified with infrared spectroscopy by Eischens *et al.* (*34*) as neutral ZnH and OH surface species. Conductivity measurements on ZnO by Wick (*35*) and by Kubokawa and Toyama (*36*) show no changes due to H_2 adsorption below about 100°C. Likewise the surface charge measurements of Enikeev *et al.* (*25*) show no net surface charge with H_2 adsorption at 20°C. Many other measurements (*37*) also show a transition temperature below which the hydrogen induced conductivity is either sharply diminished or negligible. The transition temperature, however, is sensitive to pretreatment conditions and varies in different investigations.

Dent and Kokes (*38*) presented a detailed mechanism for forming both the ZnH and OH species by reaction of repeating Zn–O groups at the surface with gaseous H_2. The overall effect, also deduced by Eischens *et al.* (*34*), may be represented by:

$$ZnO + H_2 \rightarrow ZnH + OH. \qquad (19)$$

Since both forms ZnH and OH coexist at room temperature (*34*) where there is no conductivity enhancement by hydrogen, it is likely that these are formed without charge transfer, as the Dent and Kokes (*38*) mechanism suggests. This mechanism has also received strong support from the work of Naito *et al.* (*39*).

To account for the observed increase in *n*-type conductivity produced by hydrogen adsorption at higher temperatures, several ionic forms of hydrogen chemisorption have been suggested, all capable of transferring electrons to the bulk conduction band (*34*). One of these results in hydroxyl formation:

$$H_{2_{(g)}} + 2O^{2-} \rightleftharpoons 2OH_{(ads)}^- + 2e^-, \qquad (20)$$

or

$$H_{2_{(g)}} + O^{2-} + ZnO \rightleftharpoons Zn^+ + 2OH_{(ads)}^- + e^-. \qquad (21)$$

Reasoning from the reversibility of the conductivity enhancement of ZnO on exposure to hydrogen as observed by Kubokawa and Toyama (*36*), it is assumed that Eqs. (20) and (21) are reversible reactions with reactants and products existing in equilibrium. Other proposed ionic mechanisms are more likely to be irreversible, such as the proton mechanism which leads to H^+ formation and a reduction mechanism forming H_2O on the surface (*34*).

The lack of conductivity at low temperatures presumes that the electrons generated by chemisorption at these conditions are trapped rather than released into the conduction band (*34*). A good possibility is that this trapping occurs by:

$$Zn^+ + e^- \rightleftharpoons Zn^0, \qquad (22)$$

where the Zn^+ is an ionized interstitial donor or an excess lattice cation. At low temperatures the equilibrium is shifted far to the right as shown.

The Exchange Mechanism

Omitting the details, the overall result of the Dent and Kokes mechanism is:

$$\text{ZnH} + D_2 \rightarrow \text{ZnD} + \text{HD}, \qquad (23)$$

and

$$\text{OH} + D_2 \rightarrow \text{OD} + \text{HD}, \qquad (24)$$

and similarly for ZnD and OD reacting with H_2. These mechanisms involve no overall electron transfer, which can explain the observed insensitivity to the irradiation. However, these reactions do not explain many other facts about the exchange reaction on ZnO. A satisfactory mechanism for the reaction should be able to explain:

1. The fact that at a given temperature and pressure the reaction rate *decreases* as the total number of adsorbed molecules of hydrogen and deuterium *increases*, as shown in Figs. 6 and 7.
2. The response of the reaction rate to the electronic effects induced by doping (*11*) and by adsorbing selected donor and acceptor impurities on the surface (*10*).
3. The complete absence of any photoeffects on the reaction rate or on the hydrogen chemisorption, even though this radiation increases the conductivity, enhances the CO oxidation rate, and can introduce some of the same electronic effects as doping.
4. The fact that conductivity measurements indicate that hydrogen adsorption at low temperatures is independent of electronic effects, yet the exchange rate responds to the electronic changes induced by doping at these temperatures.
5. The unusual sensitivity of the reaction to pretreatment conditions as presented in Table 3.
6. The frequent changes in slope in the Arrhenius plots as shown in Fig. 5.

It will be shown that it is possible to explain these items by proposing two methods of creating the Dent–Kokes sites. One method takes place with charge transfer and the other without.

Production of Reaction Sites

The first proposed site producing mechanism involves no charge transfer and is represented by the following surface reactions leading to nonionic species.

$$H_2 \rightarrow H + H, \qquad (25)$$

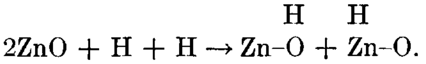

$$2\text{ZnO} + H + H \rightarrow \overset{H}{\text{Zn–O}} + \overset{H}{\text{Zn–O}}. \qquad (26)$$

The $\overset{H}{\text{Zn–O}}$ and $\overset{H}{\text{Zn–O}}$ represent the formation of the ZnH and OH Dent–Kokes sites in Eqs. (23) and (24).

A second mechanism proposed involves charge transfer and has an ionic surface species as an intermediary. This reaction may be regarded as a continuation or alternate form of Eq. (21). The electron released may react immediately with the Zn^+ to give neutral Zn^0 atoms which are mobile at the reaction temperatures. These can react further to give

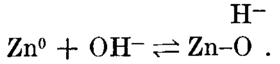

$$Zn^0 + OH^- \rightleftarrows \overset{H^-}{\text{Zn–O}}. \qquad (27)$$

The ionic $\overset{H^-}{\text{Zn–O}}$ species is considered to be completely inactive in the reaction with the hydrogen bound too tightly for the exchange to occur. However, if the electron in this species can be transferred to a trap or localized hole in the space charge region just below the surface, the result is:

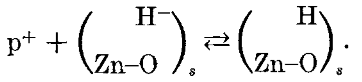

$$p^+ + \left(\overset{H^-}{\text{Zn–O}}\right)_s \rightleftarrows \left(\overset{H}{\text{Zn–O}}\right)_s. \qquad (28)$$

The holes p^+ in the space charge region are usually associated with an ionized interstitial zinc, Zn_i^+ so that Eq. (28) is equivalent to:

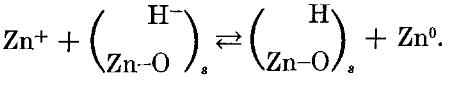

$$Zn^+ + \left(\overset{H^-}{\text{Zn–O}}\right)_s \rightleftarrows \left(\overset{H}{\text{Zn–O}}\right)_s + Zn^0. \qquad (29)$$

In Eqs. (28) or (29) an active $\overset{H}{\text{Zn–O}}$ site is created for the exchange with the equilibrium:

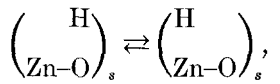

$$\left(\overset{\text{H}\diagdown}{\text{Zn–O}}\right)_s \rightleftarrows \left(\overset{\diagup\text{H}}{\text{Zn–O}}\right)_s, \qquad (30)$$

giving the mobility needed for the exchange via the Dent–Kokes mechanism. The subscript s in these equations indicates a location on the surface. Constituents without a subscript are in the space charge region.

The exact form of the species represented here by $\overset{\text{H}^-}{\text{Zn–O}}$ is, of course, unknown and cannot be specified precisely, although there is evidence for the existence of a surface OH^- group (*34*, *42*). The $\overset{\text{H}^-}{\text{Zn–O}}$ symbol merely represents some negatively charged precursor of a Dent–Kokes site which is generated by one of the several modes of hydrogen chemisorption involving hydroxyl formation and charge transfer. This species, whatever its form, can then generate an active site by further charge transfer. It is this idea of an inactive intermediate formed with charge transfer leading to an active site on further charge transfer which can explain the experimental facts in Items 1 through 6 of the discussion of the exchange mechanism.

Any form of pretreatment which produces a large positive space charge region will enhance Eq. (29) by providing more electron acceptor traps and thereby producing more Dent–Kokes sites. In this manner, the most strongly preheated catalysts which have the most negative surface and the most electropositive space charge region are the best catalysts, as shown in Table 3.

This also explains the poisoning shown in Fig. 6 which begins as soon as either hydrogen or deuterium is admitted to a freshly activated catalyst. The bands flatten during the chemisorption with electrons from Eqs. (20) and (21) filling the Zn^+ traps in the space charge region. As these traps are filled there are then fewer holes or Zn^+ ions to react in Eq. (29). The equilibrium described by this equation becomes increasingly displaced to the left, building up a higher concentration of the inactive $\overset{\text{H}^-}{\text{Zn–O}}$ species at the expense of the active $\overset{\text{H}}{\text{Zn–O}}$ sites. Without the competing type of hydrogen adsorption in the form of the $\overset{\text{H}^-}{\text{Zn–O}}$ site, the reaction rate by Eqs. (23) and (26) should increase as the total adsorption of hydrogen increases to a saturation value. As shown in Figs. 6 and 7, however, the decrease in reaction rate closely parallels the increase in total hydrogen adsorption.

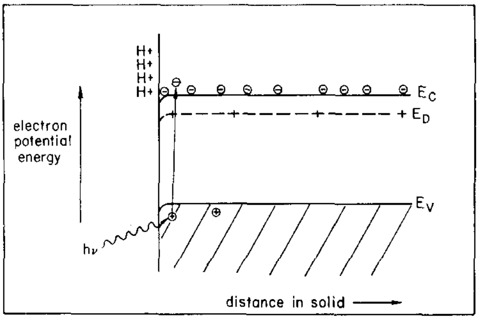

FIG. 9. Band diagram of ZnO with positively charged surface.

The Role of Additional Chemisorptive Processes

As reaction temperatures increase, more powerful chemisorption reactions become involved which possess an electrochemical potential sufficient to transfer electrons to the conduction band near the surface even after all the traps in the space charge zone have been filled. When this occurs the surface region becomes more n-type than the bulk with a higher electrical conductivity. At the reaction temperatures studied here, this conductivity increase is small (*36*) indicating that relatively few electrons from adsorbed hydrogen reach the conduction band. After the injection of only a few electrons into the already electron-rich conduction band, a negative potential builds up to oppose further electron transfer as shown in Fig. 9. This process explains the conductivity transition temperature and the breaks in the Arrhenius plot shown in Fig. 5. There is a sudden increase in the rate at which the rate constant decreases with lowering temperature. In fact, one break consistently occurs at temperatures around 100°C, the most frequently reported value for the transition between hydrogen adsorption with no conductivity effects and that which produces enhanced conductivity. At this point there is a total absence of positive charges in the space charge region so that Eq. (29) does not occur at all.

Effects of Doping and Surface Impurities

Based on the electronic processes described so far, one can now explain the results of adsorbing a small amount of oxygen on the surface before the reaction begins. Oxygen, a strong electron acceptor, creates a more negative surface and a higher degree of the band bending as shown in Fig. 8. Consequently, there is a more positive space charge region containing more traps and creating a higher $\overset{\text{H}}{\text{Zn–O}}$ concentration on the surface through Eqs. (28) or (29). The subsequent catalytic action then has a higher rate. Pretreatment with oxygen at 300°C produced a curve almost identical with Curve C in Fig. 5.

Adsorption of small amounts of water vapor has a similar effect. Water at these conditions adsorbs as an electron acceptor (*21*, *41*) but produces much less band bending than oxygen adsorption (*22*). The increase in the catalytic rate is shown by Curve C in Fig. 5 where a small amount of water vapor has been adsorbed on the catalyst. At high temperatures it shows an appreciable enhancement over the hydrogen saturated case shown in Cuve B. At low temperatures or in the presence of high water concentrations there can be physical adsorption or chemical reaction on the surface which poison the reaction.

The doping experiments of Molinari and Parravano (*11*) can be explained similarly. In catalysts doped with Li_2O a decreased *n*-type behavior was noted along with a lower reaction rate. As explained by Parravano and Boudart (*40*), the lowered *n*-type behavior is due to the fact that conduction electrons are removed to form more Zn^+ from lattice Zn^{2+} ions, but this higher concentration of Zn^+ must be maintained in both the bulk and in the space charge region to serve as charge compensation for the replacement of lattice Zn^{2+} ions with Li^+. This means that fewer Zn^+ traps in the space charge region can undergo the reaction in Eq. (29), causing a reduction of the active $\overset{\text{H}}{\text{Zn–O}}$ sites in favor of a higher concentration of the inactive $\overset{\text{H}^-}{\text{Zn–O}}$ and a *lower* reaction rate.

In a similar manner doping with a trivalent oxide such as Ga_2O_3 produces more *n*-typeness and a higher reaction rate (*11*, *40*). In this case charge compensation for the trivalent impurities requires the equilibrium in Eq. (22) to be shifted to the right to maintain a higher concentration of neutral Zn^0 interstitials. These necessary Zn^0 interstitials can also be provided by shifting Eq. (29) to the right with the accompanying increase in active $\begin{bmatrix} \text{H} \\ \text{Zn–O} \end{bmatrix}_s$ sites at the expense of the inactive $\begin{bmatrix} \text{H}^- \\ \text{Zn–O} \end{bmatrix}_s$ and subsequently a *higher* reaction rate.

Effects of Radiation

The Dent–Kokes mechanism does not involve a charge transfer so that there should be no direct effect of radiation on it. However, it is still necessary to explain the lack of any radiation effects on the concentration of the inhibiting $\overset{\text{H}^-}{\text{Zn–O}}$ sites, which definitely do involve a charge transfer. It might be argued that the incident radiation does not have sufficient intensity to alter the electronic state of the surface region enough to influence the exchange reation. However, with an ultraviolet intensity of only about one-third of that used in this study, Nobbs (*41*) found a large photoconductivity in zinc oxide. Likewise, the radiation intensity employed is ample to significantly alter the hole and electron concentrations important in the oxidation of carbon monoxide.

The lack of any effect on the OH^- formation must be explained in terms of the reaction of the electron–hole pairs created by the radiation. Although the details of the reaction may be very complex, an important feature of the proposed mechanism is that the active $\text{Zn–}\overset{H}{O}$ sites and the competing inactive $\text{Zn–}\overset{H^-}{O}$ sites coexist in an electrochemical equilibrium between surface and space charge regions with the overall stoichiometry of Eq. (29).

A photogenerated electron–hole pair has no overall effect on this equilibrium in that electrons and holes shift the reaction equally in opposite directions. During the H_2–D_2 exchange reaction the band bending at a hydrogen or deuterium saturated surface is as shown in Fig. 9. This bending does not cause any appreciable separation of the pair and produces no enhanced concentration of photogenerated holes near the surface.

This situation is very different from that in CO oxidation where the band bending is of the type illustrated in Fig. 8. In this case there is a separation of photogenerated holes and electrons by the potential gradient near the surface allowing one carrier to undergo reaction which cannot be reversed by the other. The holes which are concentrated at the surface can in this case both generate new sites and create additional reaction products by Eqs. (14)–(18) without reversal by an equal number of electrons in the surface region.

Thermal Effects of Irradiation

The possibility of confusion between true photoeffects and photothermal effects has been studied in this work. Temperature measurements showed that the catalytically important band gap radiation at an intensity of about 7 mW/cm^2, caused only transient increases in the temperature, never exceeding 1°C. Reference to the Arrhenius plot for the CO oxidation in Fig. 2 indicates that in order for the dark reaction at 30°C to achieve the same rate as with the irradiated catalyst, its temperature would have to be raised more than 200°C.

A study of irradiation effects on the ZnO catalyzed H_2–D_2 exchange showed that purposely poor filtration of infrared radiation could cause increases in temperature as large as 15°C on the catalyst surface. This could easily cause a rate increase which might be incorrectly interpreted as a photocatalytic effect.

An additional heat producing mechanism is the decay of fundamental excitations. During the time the catalyst is exposed to radiation with a photon energy greater than that of the band gap, electrons are continually being excited into the conduction band and are then continually decaying to lower energy states and to the valence band. Although most of the energy release with this decay will be in the form of reemitted electromagnetic radiation, it is accompanied by secondary scattering mechanisms which result in the production of some thermal energy. The temperature measurements at the catalyst surface in conjunction with the Arrhenius plot data permit a compensation to be calculated for the influence of these effects, although in this study they were negligible.

SUMMARY AND CONCLUSIONS

This study has illustrated a number of important concepts involved in the interpretation and experimental measurement of radiation effects on a catalyst. These are summarized below with specific application to ZnO:

1. A spectrum of reaction rate vs wavelength of the incident radiation free of

effects due to intensity variations and thermal effects indicates the specific electronic excitations important in the catalysis. On surfaces which cannot be saturated with respect to the induced photoeffects, it is necessary to measure the radiation intensity and make all measurements at the same intensity values. Likewise, it is necessary to exclude all extraneous infrared components which might accompany the radiation source. Temperature changes must be monitored at the surface of the irradiated catalyst and appropriate adjustments must be made from an Arrhenius plot to refer all measurements to a constant reaction temperature. It is the authors' conclusion that other investigations which have reported ultraviolet effects on the H_2–D_2 exchange (*9*) and on the adsorption of hydrogen (*18*) are spurious because of neglect of one of these experimental precautions.

2. For the interpretation of photocatalytic effects it is important to have as much information as possible about the electronic properties of the material and the structure of chemisorbed reaction components. Most important is the direction and magnitude of band bending in the space charge region produced by adsorption of the reactants and products. This is because of the important role of the potential differences between surface and space charge region in selectively concentrating either holes or electrons at the surface. The increased concentration of one of these at the surface may generate new surface species or "sites" for the reaction or may directly influence a surface reaction on existing sites.

3. It is important to examine photoeffects on various side reactions which may affect the principal reaction under investigation. Examples are the possible photodesorption or photoalteration of poisons. In this study no photodesorption was detected on ZnO but photoassisted alteration of the CO_2 poisoning of the CO oxidation definitely occurs.

4. It is not necessarily correct to conclude that a reaction which is not affected by radiation is totally independent of charge transfer effects and electronic state changes. As shown in the investigation of the H_2–D_2 exchange, the formation of sites for the reaction is influenced favorably by holes (electron acceptors) near the surface, which can be increased by doping or surface adsorption but not by irradiation.

5. Although the two reactions on ZnO have quite different mechanisms, they have in common an enhancement brought about by charge transfer to holes at or near the surface. In the case of the CO oxidation this hole concentration is increased by radiation of the proper frequency. In the H_2–D_2 exchange this hole concentration may be increased by doping or by certain types of pretreatment, but not by radiation. The explanation of this difference is given by the difference in band bending near the surface due to hydrogen adsorption from that produced by oxygen.

ACKNOWLEDGMENTS

The authors express their appreciation to the National Science Foundation for support of this research under Grant No. GK 12858 for Research on Radiation Effects on Solid Catalysts at Rice University. The authors are indebted to Dr. J. W. Hightower for continuous help and suggestions, to Charles J. Stone for assistance with the dark rate kinetic studies of the CO oxidation, and to W. C. Pettersen for the tracer studies showing the absence of photodesorption of CO_2.

REFERENCES

1. Harkins, C. G., Shang, W. W., and Leland, T. W., *J. Phys. Chem.* **73**, 130 (1969).
2. Doerffler, W., and Hauffe, K., *J. Catal.* **3**, 171 (1964).
3. Romero-Rossi, F., and Stone, F., *Actes Congr. Int. Catal., 2nd, 1960* **2**, 1481 (1961).
4. Tanaka, K., and Blyholder, G., *J. Phys. Chem.* **76**, 1807 (1972).
5. Nagarjunan, T. S., and Calvert, J. G., *J. Phys. Chem.* **68**, 17 (1964).
6. Lyashenko, L. V., and Gorokhovatskii, Y. B., *Theor. Exp. Chem.*, (*USSR*) **3**, 218 (1967).
7. Schwab, G., Noller, H., Steinbach, F., and Venugopalan, M., *Nature* **193**, 774 (1962).

8. Steinbach, F., *Z. Phys. Chem.* **60**, 126 (1968).
9. Freund, T., *J. Catal.* **3**, 289 (1964).
10. Clark, A., *Ind. Eng. Chem.* **45**, 1476 (1953).
11. Molinari, E., and Parravano, G., *J. Amer. Chem. Soc.* **75**, 5233 (1953).
12. Stone, C., MS thesis, Rice Univ., 1970.
13. Chizhikova, G. I., *Kinet. Catal.* **7**, 616 (1966).
14. Schwab, G., and Block J., *Z. Phys. Chem.* **1**, 42 (1954).
15. Gobrecht, H., Hahn, D., and Scheffler, K., *Z. Phys.* **139**, 365 (1954).
16. Scharowsky, E., *Z. Phys.* **135**, 318 (1953).
17. Fulkerson, W., and Leland, T. W., *J. Catal.* **2**, 87 (1963).
18. Kesavulu, V., and Taylor, H. A., *J. Phys. Chem.* **66**, 54 (1962).
19. Mollwo, E., *Z. Angew Phys.* **6**, 257 (1954).
20. Rubin, T. R., Calvert, J. G., Rankin, G. T., and MacNevin, W. M., *J. Amer. Chem. Soc.* **75**, 2850 (1953).
21. Veerkamp, T. F., PhD thesis, Rice Univ., 1973.
22. Murphy, W. R., Veerkamp, T. F., and Leland, T. W., to be published.
23. Sancier, K. M., *J. Catal.* **9**, 331 (1967).
24. Amigues, P., and Teichner, S. J., *Discuss. Faraday Soc.* **41**, 362 (1966).
25. Enikeev, E. K., Margolis, L. Y., and Roginskii, S. Z., *Dokl. Akad. Nauk., USSR* **118**, 85 (1958).
26. Komatsu, W., Naka, O. I., and Kobayashi, R., *J. Catal.* **15**, 43 (1969).
27. Chon, H., and Prater, C. D., *Discuss. Faraday Soc.* **41**, 380 (1966).
28. Amberg, C. H., and Seanor, D. A., *J. Chem. Phys.* **42**, 2967 (1965).
29. Lunsford, J. H., and Jayne, J. P., *J. Chem. Phys.* **44**, 1487 (1966).
30. Barry, T. I., and Stone, F. S., *Proc. Roy. Soc. A* **255**, 124 (1960).
31. Matsushita, S., and Nakata, T., *J. Chem. Phys.* **36**, 665 (1962).
32. Pettersen, W. C., MS thesis, Rice Univ., 1973.
33. Stone, F. S., *in* "Advances in Catalysis" (D. D. Eley, P. W. Selwood and P. B. Weisz, Eds.), Vol. 13, p. 1, Academic Press, New York, 1962.
34. Eischens, R. P., Pliskin, W. A., and Low, M. J. D., *J. Catal.* **1**, 180 (1962).
35. Wick, E., *Z. Elektrochem.* **53**, 279 (1949).
36. Kubokawa, Y., and Toyama, O., *J. Phys. Chem.* **60**, 833 (1956).
37. Cimino, A., Molinari, E., Cramarossa, F., and Ghersini, G., *J. Catal.* **1**, 275 (1962).
38. Dent, A. L., and Kokes, R. J., *J. Phys. Chem.* **73**, 3781 (1969).
39. Naito, S., Shimizu, H., Hagiwara, E., Onishi, T., and Tamaru, K., *Trans. Faraday Soc.* **67**, 1519 (1971).
40. Parravano, G., and Boudart, M., *in* "Advances in Catalysis," (W. G. Frakenburg, V. I. Komarewsky and E. K. Rideal, Eds.), Vol. 7, p. 47. Academic Press, New York, 1955.
41. Nobbs, J. M., *J. Phys. Chem. Solids* **29**, 439 (1968).
42. Dowden, D. A., and Mackenzie, N., *Proc. Roy. Soc. A* **237**, 245 (1956).